Advances in aberration corrected STEM at ORNL

A. R. Lupini, M. Varela, A. Y. Borisevich, S. M. Travaglini and S. J. Pennycook
Condensed Matter Sciences Division, Oak Ridge National Laboratory, Oak Ridge, TN 37831-6031

Abstract. Aberration correction has recently made the transition from being merely a technically interesting result to finally becoming a practical tool for extremely high resolution electron microscopy. In this paper we discuss some of the progress that is being made and highlight some of the more unexpected advantages that aberration correction will bring.

1. Introduction

For many years, the optical aberrations of the round lenses have determined the primary resolution limit in most high-performance transmission electron microscopes (TEMs). The proof in 1936 by Scherzer that the spherical (C_s) and chromatic aberration (C_c) will always have positive values for conventional round lenses seemed to set a limit on the performance that can be achieved with any realistic pole-piece design [1]. Attempts to minimize these aberrations have contributed significantly to the present state-of-the-art in TEM and result in limited space available for insertion, in-situ treatment and tilt of the sample. It is therefore not surprising that there have been many attempts to correct the spherical aberration of the objective lens [2]. However, it is only in recent years that spherical aberration correctors have actually improved the resolution of the microscope on which they are fitted. Reasons for the lack of success include stringent stability requirements, but are largely due to the difficulty of aligning such a system. It is no coincidence that all of the successful aberration correctors rely on sophisticated computer control to automate this procedure [3].

One sign that C_s-correction has come of age is that plans for more modern correctors are already going beyond just considering spherical aberration and are tackling higher order aberrations [4,5]. It is hoped that fifth order correctors will provide a further reduction in probe size over the current generation of C_s-corrected systems.

With the geometric lens aberrations corrected, the next limiting factor is likely to be chromatic aberration. It is normally assumed that the defocus spread, Δf, from chromatic aberration depends on the instabilities and energy spread added in quadrature:

$$\Delta f = C_c \left(2\frac{\Delta I}{I} \right)^2 + \left(\frac{\Delta V}{V} \right)^2 \Bigg)^{1/2}$$

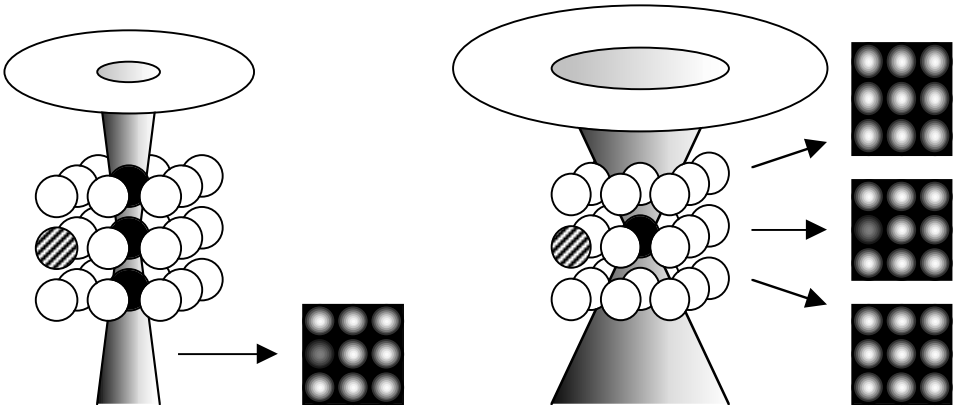

Figure 1. Schematic of the effect of changing aperture size in a model system without channeling. A single dopant atom is shaded. For a small aperture (left), a whole column is illuminated with similar intensities, and so the single image is a projection of the structure. As the aperture size increases (right), the depth of field is decreased, so a series of images is generated at different focal planes.

Where ΔI represents the fluctuations in the lens current, I, and ΔV represents the energy spread of electrons due to both the range of energies from the tip and instabilities, particularly in the high voltage supply, V. Assuming that the fractional instabilities in the lens currents can be kept below 1 part per million (ppm), and the energy spread is of the order of 1-2 ppm from a cold field emitter at 100-300 keV, the range of focus values due to chromatic effects will be approximately 3 nm. This result is a major factor in the information limit of a TEM, and suggests that the high angle annular dark field (HAADF) imaging mode of a scanning transmission electron microscope (STEM) with its reduced sensitivity to C_c [6] provides an attractive site for a pure C_s-corrector. Possible solutions to this problem would include either monochromation or C_c-correction.

2. Three-Dimensional Atomic Resolution STEM

Another extremely interesting prospect for aberration correction is three-dimensional atomic resolution. Harnessing this capability strongly relies on selecting the appropriate objective aperture. The choice of objective aperture size in TEM or STEM is a compromise between the diffraction limit, favoring a larger aperture, and the lens aberrations which necessitate a smaller beam-defining aperture. The resolution increase obtained through aberration correction arises because correcting the geometric aberrations allows the objective aperture size to be increased, resulting in a corresponding improvement in the diffraction limit. Increasing the objective aperture size will result in a \decrease in the depth of field in a STEM. This has been shown by many authors, for example [7], who demonstrate that the increased probe intensity on nearby columns will result in some signal being detected from atoms in neighboring columns for a particular probe position. However, we suggest that the reduced depth of field could really be a significant advantage because it may allow the 3-dimensional location of a single dopant atom or vacancy. This is schematically illustrated in figure 1 for the model case of a system without channeling or aberrations.

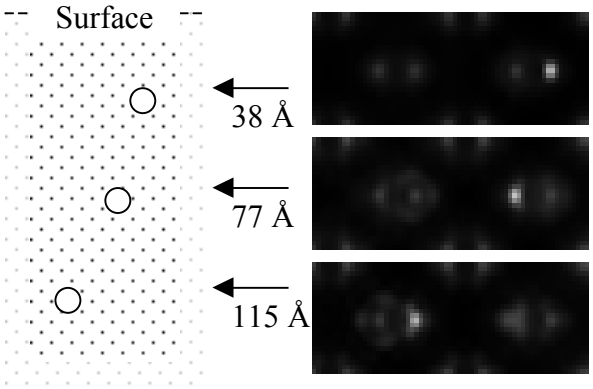

Figure 2. Simulated HAADF images of Bi atoms embedded in a 160 Å thick Si crystal viewed down the [110] axis. The Bi atoms are situated at roughly 38 Å depth steps within the crystal (left). The HAADF images generated for the probe focused at the depth of each dopant in turn are shown (right) for a 35 mrad objective aperture.

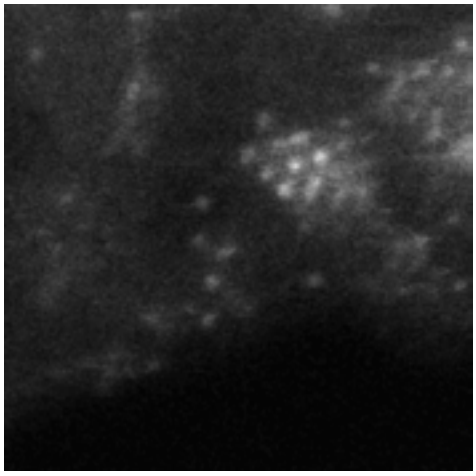

Figure 3. Experimental HAADF image of Au atoms on titania taken at 300 kV. The light titania appears as a grey background. The heavy Au atoms show up as bright spots. Both single Au atoms and clusters are visible.

We can construct a very simple estimate for the (incoherent) depth of field by considering the probe propagating in the absence of channeling and aberrations. If we assume that the diffraction limit, r_d, and the geometric spreading, r_g. given by:

r_d=0.61_/_ and r_g=z_

add approximately in quadrature, then the total probe size, r_t, is given by:

$$r_t^2 \approx r_d^2 + r_g^2 = 0.61^2 \lambda^2 / q^2 + z^2 q^2 .$$

where _ is the electron wavelength and _ is the objective aperture half-angle. If the current density is proportional to the illuminated area, then we might use the points at which the area is twice the diffraction limited value, to estimate the point at which the probe intensity is halved, giving the depth of field as: $\Delta z = 1.22 \lambda / q^2$.

Thus at 100kV, for the uncorrected case, with an objective aperture semi-angle of approximately 10 mrad, we have a depth of field of around 45 nm, which is rather too large to be useful in most cases. However, if we consider the C_s-corrected case at 300 kV, and 25 mrad, then the depth of field by this estimate is reduced to around 4 nm. This has already been shown to allow La atoms on the top and bottom of a catalyst support to be differentiated [8]. Another doubling of the aperture angle, for instance by C_5-correction, would allow sub-nm resolution for a suitable sample. Simulations indicate that extremely large aperture angles (approaching 100 mrad) should allow the detection of single dopant atoms with atomic depth resolution, depending on the material. At present, it appears this would be limited by the chromatic effects described above, and would present formidable challenges in terms of stability.

Figure 2 shows the output from a multislice calculation, performed with phonons, but with zero chromatic aberration. This shows a silicon sample doped with several bismuth atoms, viewed down the [110] axis. For suitably thin, aligned specimens, the channeling generally enhances the electron density on atomic columns, with a maximum that can (perhaps surprisingly) exceed the intensity in the free-space probe. As the crystal

becomes thicker, this intensity will oscillate, as has been described by several authors [7]. Thus there is a strong depth dependence of the intensity in the image, but this is dominated by the channeling effects rather than defocus.

However, at large enough aperture angles, the geometrical probe convergence becomes more significant and it is possible to focus the probe at variable depths within the crystal. A simple explanation is that rays at larger angles to the optic axis are, by definition, also a long way from the strong channeling condition of an aligned crystal. In the example shown in Figure 2, by focusing the probe at different depths it is possible to determine the dopant depth directly. The out of focus dopants still give a significant contribution to the image, but there is a very clear increase in intensity when the probe is focused at the depth of a particular dopant atom. We therefore also suggest that interstitial dopants will become more visible with increasing aperture size.

3. Discussion and future directions

Other work presently underway involves more detailed image simulation [9], accurate structure calculations [10], statistically justified reconstruction of experimental images [11], and further work on improving the spectrometer resolution and efficiency [5]. Single atom detection and even spectroscopy is becoming a regular occurrence, both in the bulk of a material [12] [13] and on the surface of catalyst supports [8] (or figure 3). In this paper, we have shown that with a large enough convergence angle, under suitable conditions, the 3-dimensional location of single dopant atoms appears to be theoretically feasible, although further instrumental development remains necessary.

Research sponsored by the Laboratory Directed Research and Development Program of Oak Ridge National Laboratory managed by UT-Battelle, LLC for the U.S. Department of Energy under contract No. DE-AC05-00OR22725, and by appointment to the ORNL Postdoctoral Research Program administered jointly by ORNL and ORISE.

References

[1] Scherzer O 1936 *Zeit. Phys.* **101** 593-603.
[2] Summarized by: Hawkes P W and Kasper E 1989 *Principles of Electron Optics* (Academic Press, London).
[3] Dellby N, et al. 2001 *J. Electron. Microsc.* **50** 177-185.
[4] Krivanek O L, et al 2003 *Ultramicroscopy* **96** 229-237.
[5] Nellist P D, et al 2003 *these proceedings*.
[6] Nellist P D, Pennycook S J 1998 *Phys Rev Lett* **81** (19): 4156-4159.
[7] Dwyer C, Etheridge J 2003 *Ultramicroscopy* **96** (3-4) 343-360.
[8] Borisevich A Y, et al 2003 *Proceedings Microscopy and Microanalysis 2003* (Cambridge University Press, New York).
[9] Allen L J, et al 2003, *Phys Rev Lett, to be published*.
[10] Pennycook S J, et al. *Encyclopedia of Materials: Science and Technology* (Elsevier Science Ltd) 1-14.
[11] See http://www.pixon.com.
[12] Varela M, et al 2003 *in preparation*.
[13] Lupini A R, Pennycook S J 2003 *Ultramicroscopy* **96** (3-4) 313-322.